ISSN:2790-1688 Volume-14-(2025)

The research of new water electrolysis catalysts: Co(OH)x-NiFeP/NF

Jiayi Du

The department of chemistry, University College London, London WC1E 6BT, Britain

zccajdu@ucl.ac.uk

Abstract. Developing efficient and durable bifunctional catalysts for water electrolysis under high current densities (HCD) is essential for sustainable energy systems. This research synthesized a hierarchical Co(OH)x-NiFeP/NF catalyst with a crystalline-amorphous interface via electrochemical deposition. Scanning and transmission electron microscopy (SEM/TEM) revealed a unique nanostructure characterized by nanoneedles coated with amorphous $Co(OH)_x$, optimizing surface roughness and active site exposure. Electrochemical measurements demonstrated outstanding OER performance, the overpotential of $Co(OH)_x$-NiFeP/NF achieving 285 mV at 200 mA cm^{-2} and 357 mV at 1000 mA cm^{-2}, significantly outperforming NiFeP/NF and $Co(OH)_x$/NF. The catalyst exhibited a low Tafel slope (84 mV dec^{-1}) and superior intrinsic activity with a turnover frequency (TOF) of 0.87 s^{-1} at 300 mV. Furthermore, EIS results indicated minimal charge transfer resistance (1.185 Ω), and durability testing confirmed stable operation over 200 hours at high current densities. Co(OH)x-NiFeP/NF also performs well when integrated into a complete water-splitting system, surpassing most reported bifunctional catalysts. This work demonstrates the potential of $Co(OH)_x$-NiFeP/NF as an economically benefit and resizable catalyst for high-performance water electrolysis.

Keywords: NiFeP; water splitting; OER; interface.

1. Introduction

The growing demand for sustainable energy solutions has led to various research in hydrogen production through water electrolysis, a potential technology for sustainable new energy reserves. Alkaline water electrolysis has gained considerable attention because it can operate using non-precious metal-based catalysts, making it an economical and efficient alternative to proton exchange membrane (PEM) electrolyzers. However, Nowadays, a key challenge is to develop more efficient and serviceable catalysts for the oxygen evolution reaction (OER) that can work at high current densities (HCD). Therefore, we must find advanced catalysts with higher activity, stability and scalability.[1]

Transition metal-based electrocatalysts, such as nickel-iron phosphides (NiFeP) and cobalt hydroxides ($Co(OH)_x$), Because of their adjustable electronic structure and abundant active sites, they are considered as a potential research direction. However, catalytic efficiencies at high current densities are often not ideal because they are limited by poor charge transfer, structural instability, and insufficient exposure to the active site. This suggests that these materials still need to be further optimized.[2]

In recent years, researchers have made significant progress in enhancing the electrocatalytic properties of transition metal-based materials by optimizing nanostructures, doping and heterostructural engineering. For example, NiFeP catalysts exhibit excellent intrinsic activity, while amorphous $Co(OH)_x$ has excellent stability and surface reactivity. Therefore, combining crystalline and amorphous phases and using the advantages of these two structures to form entirely new materials is a promising strategy.[3-4]

However, some challenges remain, especially in achieving low overpotential and maintaining stability at high current densities. Limitations on the interfacial interaction between the two phases make it challenging to design effective bifunctional catalysts. Therefore, there is an urgent need for innovative material architectures to enhance charge transfer dynamics, improve structural durability, and optimize exposure to active sites.

In this study, we propose a novel layered $Co(OH)_x$-NiFeP/NF catalyst with the crystal-amorphous interface, which is synthesized by hydrothermal treatment, phosphorylation and electrodeposition. This design combines the advantages of crystalline NiFeP and amorphous $Co(OH)_x$ for improved catalytic activity and durability. The nanomedle form of the base, coated with an amorphous hydroxide shell, improves charge transfer, increases electrochemical surface area (ECSA) and enhances structural stability. After experimental analysis, our heterostructure has excellent oxygen evolution (OER) performance, with an overpotential of 285 mV at 200 mA cm ($^{-2}$), exceeding that of conventional catalysts. It also exhibits a low Tafel slope of 84 mV dec-1 and a high turnover frequency (TOF).

When integrated into a complete water decomposition system, the $Co(OH)_x$-NiFeP/NF catalyst can achieve a battery voltage of 1.62 V at 100 mA cm^{-2}, superior to many bifunctional catalysts. Electrochemical impedance spectroscopy (EIS) shows the most minor charge transfer resistance (1.185Ω). In durability tests, it has been shown to operate stably for more than 200 hours at high current densities. These data highlight the catalytic efficiency of the catalyst and provide insights into how advanced electrocatalysts for sustainable hydrogen production can be developed, initially addressing the challenges of water electrolysis at high current and density conditions and offering promising solutions for large-scale energy conversion.

2. Experimental Section

2.1 Materials and Reagents

Nickel foam (Ni, ⩾99.9%) with excellent electrical conductivity and a three-dimensional porous structure was obtained from Kunshan Guangjiayu Material Co., Ltd. as the electrocatalyst loading substrate. To enhance its surface wettability, sodium dodecyl sulphate ($C_{12}H_{25}SO_4Na$, analytically pure) purchased from McLean Biochemical Technologies Co., Ltd. was employed for hydrophilic treatment. Ferric nitrate ($Fe(NO_3)_3·6H_2O$, analytically pure) and nickel nitrate hexahydrate ($Ni(NO_3)_2·6H_2O$, analytically pure) were sourced from Beijing Chemical Factory and utilized as iron, cobalt, and nickel precursors in the synthesis of $Co(OH)_x$ and NiFeP. Additionally, ammonium fluoride (NH_4F, analytically pure) and urea ($CO(NH_2)_2$, analytically pure) obtained from the same supplier were used to regulate the reaction environment in hydrothermal synthesis and act as a nitrogen source and reducing agent, respectively. Sodium hypophosphite monohydrate ($NaH_2PO_2·H_2O$, analytically pure) was employed as the phosphating agent to convert precursors into phosphides. Ferric chloride ($CoCl_3$, analytically pure) was used in the electrodeposition process to synthesize $Co(OH)_x$. Acetone (C_3H_6O, analytically pure) and anhydrous ethanol (CH_3CH_2OH, analytically pure), both obtained from Beijing Chemical Factory, were utilized for cleaning and dispersion. Furthermore, 3M hydrochloric acid (HCl, analytically pure) was purchased from MOLEKULA company for surface treatments. Electrolytes and pH regulators, including potassium hydroxide (KOH, analytically pure) and sodium hydroxide (NaOH, analytically pure), were supplied by Fuchen Chemical Reagent Co., Ltd. A phosphate buffer solution (1 M K_2HPO_4 and KH_2PO_4) was obtained from Xiamen Hibo Technology Co., Ltd. and used for electrochemical measurements and turnover frequency (TOF) calculations. A commercial RuO_2 catalyst served as a reference material for performance evaluation. All experimental procedures used deionized water to ensure solution purity and minimize contamination.

2.2 Hydrophilic Treatment of Ni Foam

Before experimentation, nickel foam sheets were cut into 1.0 cm × 1.2 cm pieces using precision scissors. Care was taken to ensure uniform dimensions and clean edges. Before use, the nickel foam was inspected to confirm the absence of physical defects or surface deterioration. Then, the nickel foam (dimensions: 1 cm × 1.2 cm) was subjected to a hydrophilic pretreatment process. Initially, the Ni foam was rinsed with acetone for 5 minutes to remove surface oxides, followed by immersion in

a 3 M HCl solution within a 10-minute ultrasonic bath. The researcher subsequently used ethanol and distilled water to wash the foam.

A 3 g/L sodium dodecyl sulphate (SDS) solution was prepared by dissolving 150 mg of SDS powder with deionized water in a 50 mL volumetric flask, ensuring complete dissolution through stirring. The pretreated Ni foam was placed and wholly immersed in the SDS solution and incubated in a water bath at 90 ° C for 2 hours under continuous stirring. Following the reaction, the Ni foam was rinsed multiple times with deionized water to remove residual SDS and vacuum-dried to eliminate moisture.

2.3 Synthesis of Co(OH)x-NiFeP/NF via Hydrothermal Treatment, Phosphorization, Electrodeposition

To synthesize $Co(OH)_x$-NiFeP/NF, dissolve 0.350 g of $Fe(NO_3)_3 \cdot 6H_2O$ (1 mmol), 0.060 g of $CO(NH_2)_2$ (1 mmol), 0.145 g of $Ni(NO_3)_2 \cdot 6H_2O$ (0.5 mmol), and 0.046 g of NH_4F (2 mmol) in 17.5 mL of deionized water while continuously stirring until fully dissolved. Next, place the hydrophilic-treated nickel foam into a Teflon-lined autoclave and add the prepared solution to immerse the foam completely. Seal the autoclave and heat it to 100 °C for 16 hours. After the heating period, allow the autoclave to cool naturally to room temperature. Finally, deionized water was used to wash the foam and dry the foam in a vacuum.

For phosphorization, 0.4 g $NaH_2PO_2 \cdot H_2O$ was weighed and placed at the front of a porcelain boat, while the hydrophilic-treated Ni foam was placed at the rear. The assembly was inserted into a tube furnace, which was purified with nitrogen at 10 mL/min. The furnace was heated to 300 °C at 2 °C/min. After the heating process, the NiCoP/NF catalyst was obtained.

A 0.05 M $CoCl_3$ solution was prepared by dissolving $CoCl_3$ in deionized water. The Ni foam (working electrode), Hg/HgO (reference electrode), and a graphite rod (counter electrode) were installed in an electrochemical workstation. Electrodeposition was performed at -1.0 V (vs. Hg/HgO) for 20 minutes. After deposition, the foam was rinsed with deionized water and vacuum-dried, yielding $Co(OH)_x$-NiFeP/NF.

Synthesis of Co(OH)x/NF via Electrodeposition

A 0.05 M $CoCl_3$ solution was prepared by dissolving $CoCl_3$ in deionized water. The setup included a hydrophilic-treated nickel foam (working electrode), a mercury/mercury oxide (Hg/HgO) electrode as the reference and a graphite rod as the counter electrode. Electrodeposition was conducted at -1.0 V (versus Hg/HgO) for 20 minutes. After the deposition process, the foam was rinsed with deionized water and vacuum-dried, resulting in $Co(OH)_x$/NF.

Synthesis of NiFeP/NF via Hydrothermal Treatment, Phosphorization

To synthesize NiFeP/NF, firstly, dissolve 0.350 g of Fe(NO3)3·6H2O (1 mmol), 0.060 g of $CO(NH_2)_2$ (1 mmol), 0.145 g of $Ni(NO_3)_2 \cdot 6H_2O$ (0.5 mmol), and 0.046 g of NH_4F (2 mmol) in 17.5 mL of deionized water while stirring continuously until fully dissolved. Place the hydrophilic-treated nickel foam in a Teflon-lined autoclave and add the prepared solution to immerse the foam completely. Seal the hydrothermal reactor and heat it to 100 °C for 16 hours. After heating, allowing it to cool naturally to room temperature, wash the foam with deionized water and dry it under vacuum.

Then, applying phosphorization, weigh 0.4 g of $NaH_2PO_2 \cdot H_2O$ and place it at the front of a porcelain boat. Position the hydrophilic-treated nickel foam at the rear. Insert the assembly into a tube furnace purged with nitrogen at 10 mL/min. Heat the stove to 300 °C at 2 °C/min. After the heating process is complete, the NiFeP/NF catalyst will be obtained.

2.4 Electrochemical Characterization and Structural Analysis of Catalysts

The catalysts underwent electrochemical tests using different measurement techniques. The Linear Sweep Voltammetry measurements were done in 1 M KOH electrolyte at an electrochemical speed of 1 mV/s to examine oxygen evolution reaction (OER) activities by studying overpotential together with current density. Chonoamperometry tested stability by applying a single potential across the catalyst in 1 M KOH electrolyte as it recorded current changes during the monitoring period.

Electrochemical Impedance Spectroscopy (EIS) determined charge transfer resistance alongside capacitance properties and electrochemical surface area (ECSA) evaluation used cyclic voltammetry (CV) with scan rates between 1 to 10 mV/s to obtain double-layer capacitance (Cdl) values. For structural analysis of the catalyst, SEM enabled a thorough evaluation of its surface morphology alongside particle size distribution. The elemental breakdown of the sample came from testing it with Energy-Dispersive X-ray Spectroscopy (EDX). Operations based on HRTEM and SAED facilities enabled researchers to study both microstructural features and crystallographic properties of the material. Phase and crystal structure data collection occurred by using X-ray diffraction (XRD) with Co K α radiation through pattern reference and matching analyses.

3. Results and discussion

The morphological characteristics of the as-prepared $Co(OH)_x$/NF, NiFeP/NF, and $Co(OH)_x$-NiFeP/NF samples were investigated by scanning electron microscopy (SEM), as shown in Fig. 1. Notably, both NiFeP/NF and $Co(OH)_x$-NiFeP/NF exhibited sea-urchin-like architectures, suggesting a unique structural feature beneficial for electrocatalytic applications. For the $Co(OH)_x$/NF sample (Fig. 1a), the $Co(OH)_x$ layer was deposited onto the nickel foam (NF) substrate via electrodeposition, forming nanosheet-like structures that adhered uniformly to the NF surface. Unlike the other samples, the $Co(OH)_x$/NF surface appeared relatively smooth, indicating a simpler microstructure. In contrast, the NiFeP/NF sample (Fig. 1b) displayed vertically interconnected needle-like structures anchored on the NF surface. This morphology, characterized by the nanoneedles' highly oriented and interconnected nature, is expected to enhance the active surface area and facilitate mass transport during catalytic processes. Interestingly, the $Co(OH)_x$-NiFeP/NF sample (Fig. 1c), obtained through further electrodeposition on the NiFeP/NF substrate, demonstrated a significantly altered sea-urchin-like morphology. The cluster size of the sea-urchin structures was slightly reduced compared to that of NiFeP/NF, and the individual nanoneedles exhibited blunt tips with multidirectional orientations. These morphological changes indicate the growth of flower-like nanostructures, which increase the material's roughness and specific surface area. This structure is expected to provide more active sites for electrochemical reactions, thereby improving electrocatalytic performance.

Overall, the morphology of $Co(OH)_x$-NiFeP/NF combines the advantageous characteristics of nanosheets and nanoneedles, and this layered structure, combined with nanoscale roughness and high specific surface area, contributes to its catalytic performance and is particularly beneficial for optimizing the catalytic activity of the material in energy-related applications.[5]

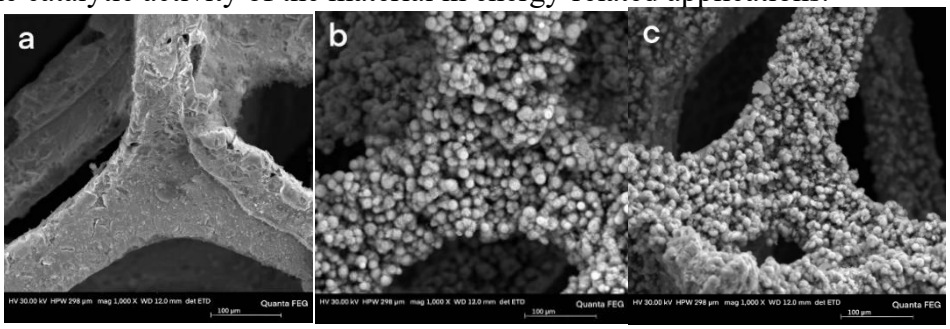

Fig. 1. SEM images of (a) $Co(OH)_x$/NF, (b) NiFeP/NF, and (c) $Co(OH)_x$-NiFeP/NF.

Transmission electron microscopy (TEM) analysis provided detailed insights into the microstructure characteristics of $Co(OH)_x$/NF, NiFeP/NF, and Co(OH) X-NiFeP /NF (Figure 2). TEM images of $Co(OH)_x$/NF (Figures 2a, b) show smooth nanosheets uniformly attached to the surface of nickel foam (NF). Alternating dark and bright areas in these images can be attributed to the folding and creasing of the ultra-thin nanosheets. This simple structure indicates that $Co(OH)_x$ is uniformly deposited on the substrate, resulting in a relatively flat structure. In contrast, NiFeP/NF displayed a more complex morphology, as shown in Fig. 2c,d. The TEM images of this sample exhibited rough surfaces with interlaced, nanoneedle-like structures. These densely distributed needle arrays create a hierarchical network that enhances surface roughness and potentially increases the

number of exposed active sites, which is beneficial for electrocatalytic applications. The $Co(OH)_x$-NiFeP/NF sample exhibited a hybrid structure that combined features of nanosheets and nanoneedles (Fig. 2e,f). The nanoneedles had rough surfaces and were partially coated with nanosheets, creating a unique composite architecture. Dark and bright regions, corresponding to the folded nanosheets, were visible, indicating the integration of $Co(OH)_x$ into the NiFeP framework. Notably, the nanoneedles displayed a core-shell structure, with poorly crystalline NiFeP cores enveloped by an outer oxide shell that contained phosphates and electrodeposited Fe hydroxides. High-resolution TEM (HRTEM) images (Fig. 2g,h) further elucidated the crystalline-amorphous dual-phase nature of $Co(OH)_x$-NiFeP/NF. An obvious interface between the crystalline and amorphous regions was observed, confirming the mixed-phase composition of the material.

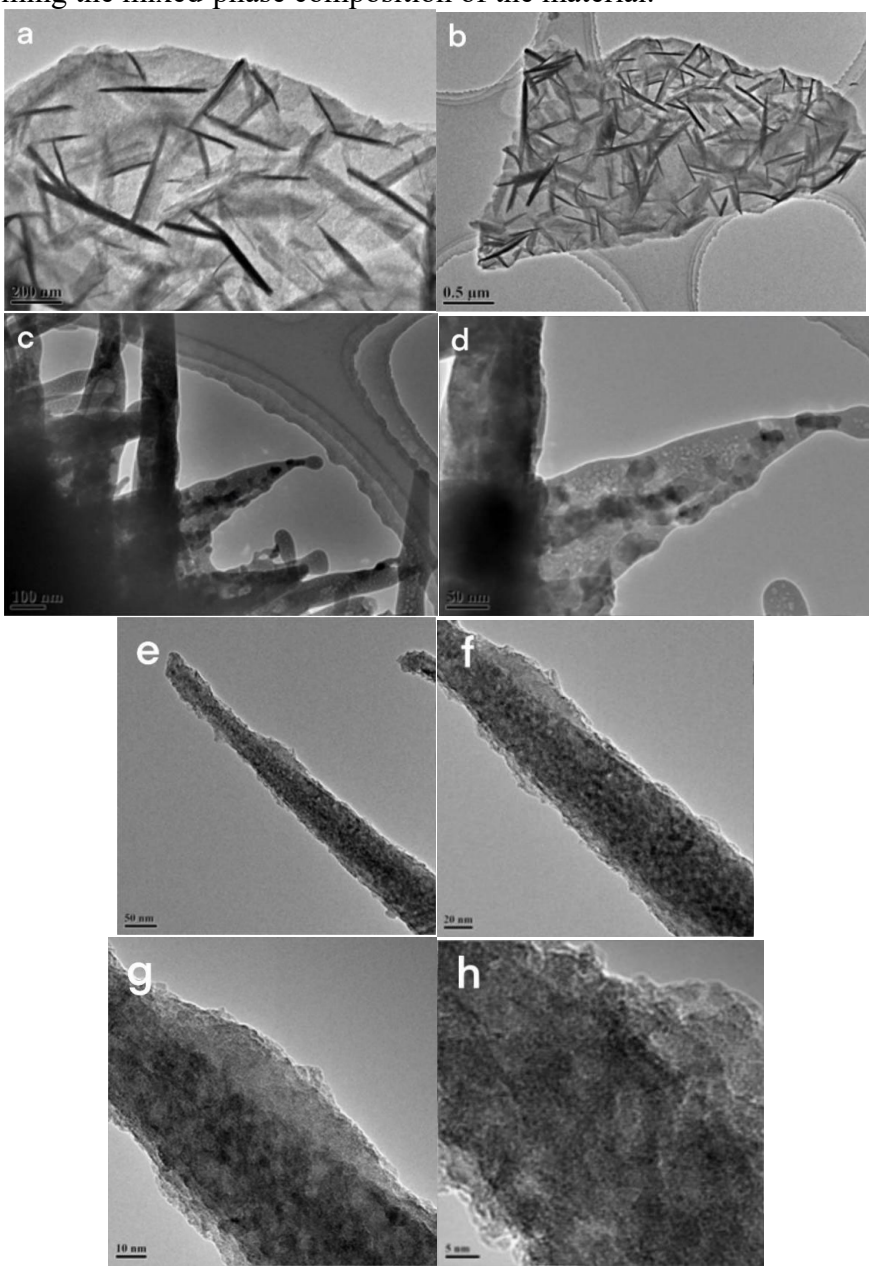

Fig. 2. TEM and HRTEM images of (a,b) $Co(OH)_x$/NF, (c,d) NiFeP/NF, and (e,f) $Co(OH)_x$-NiFeP/NF, including FFT patterns and magnified lattice fringe analysis(g,h).

In XRD data (Fig. 3), the strongest diffraction peaks of 44.4°, 51.8° and 76.4° correspond to nickel foam, indicating the presence of nickel foam base. The diffraction peaks of single-component NiFeP/NF at 41.0° and 47.6° match the (111) and (210) crystal faces of NiFeP, but the intensity is low, indicating that NiFeP has a certain crystallinity. In contrast, the diffraction peaks of $Co(OH)_x$-NiFeP/NF catalysts are wider, and their intensities decrease at 41.0° and 47.6°, indicating that the

introduction of $Co(OH)_x$ may reduce the crystallinity of NiFeP. The spiny diffraction peaks of XRD indicate that the catalyst with low crystallinity and subtle structure has been successfully prepared, which is consistent with the crystal/amorphous mixed structure observed by scanning transmission electron microscopy (STEM). It is further confirmed that the synergistic effect of $Co(OH)_x$ and NiFeP may lead to local amorphous, thereby improving the electrocatalytic performance. [5-6]

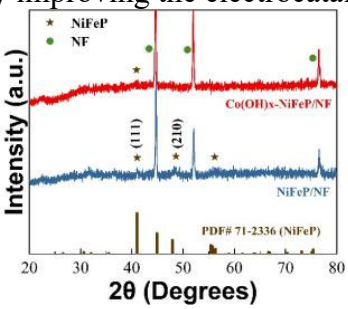

Fig. 3. The XRD peak graph for $Co(OH)_x$-NiFeP/NF,and NiFeP/NF

The electrocatalytic performance of the OER was systematically evaluated for three catalysts: $Co(OH)_x$-NiFeP/NF, NiFeP/NF, and $Co(OH)_x$/NF, as illustrated in Figure 4. The polarization curves displayed in Figure 4a illustrated that $Co(OH)_x$-NiFeP/NF exhibited the lowest overpotential at 285 mV under the condition of current density for 200 mA cm^{-2}, outperforming both NiFeP/NF (347 mV) and $Co(OH)_x$/NF (359 mV). As the applied voltage increased, the current density of $Co(OH)_x$-NiFeP/NF showed a significantly greater rate of increase compared to the other catalysts, demonstrating its superior catalytic efficiency. Notably, at a current density of 500 mA cm^{-2}, $Co(OH)_x$-NiFeP/NF maintained a low overpotential of 319 mV, which is substantially lower than that of NiFeP/NF (426 mV) and $Co(OH)_x$/NF (410 mV). Even at ultra-high current densities of 1000 mA cm^{-2}, the overpotential of $Co(OH)_x$-NiFeP/NF remained at 357 mV, significantly better than $Co(OH)_x$/NF (475 mV). This highlights its remarkable stability and efficiency for high-rate OER applications. Further insights into the catalytic kinetics were obtained from the Tafel plots. At a lower current density of 200 mA cm^{-2} (Figure 4b), $Co(OH)_x$-NiFeP/NF exhibited the lowest Tafel slope of 84 mV dec^{-1}, showing favourable reaction kinetics performance. This suggests minimal energy loss and a gradual increase in overpotential with rising current density. The stability in Tafel slopes across different current densities reflects the material's efficient charge transfer and robust catalytic performance under challenging conditions. To evaluate the electrochemical active surface area (ECSA) further, the capacitance of the double-layer (Cdl) was measured (Figure 4c). The $Co(OH)_x$-NiFeP/NF catalyst displayed a significantly higher Cdl value of 261.66 mF cm^{-2}, far exceeding those of NiFeP/NF and $Co(OH)_x$/NF, indicating a much larger ECSA. The high Cdl value, combined with its superior catalytic kinetics, suggests that the hierarchical structure of $Co(OH)_x$-NiFeP/NF provides abundant active sites, facilitating efficient mass and charge transfer. These results confirm that the cooperative effect of the crystalline-amorphous structure and the unique core-shell architecture of $Co(OH)_x$-NiFeP/NF greatly enhances its OER catalytic performance, particularly under high current densities, making it a potential candidate for large-scale energy production systems.[5-7]

Ruthenium oxide (RuO_2) is a highly efficient catalyst for the OER, commonly worked under acidic water electrolysis systems. Experimental data (Figure 4 d,e) indicate that RuO_2 has an overpotential of approximately 480 mV(versus the reversible hydrogen electrode, RHE) at a current density of 200 mA cm^{-2}. This low energy loss greatly surpasses many other transition metal oxide catalysts and demonstrates its high catalytic activity. Additionally, RuO_2 features a Tafel slope of about 75 mV dec^{-1} , suggesting that the kinetics of the OER are rapid, with an efficient electron transfer process. As a result, RuO_2 can deliver a high current density at a low overpotential, enhancing the overall efficiency of water decomposition. The exceptional catalytic activity of RuO_2 is primarily attributed to the REDOX cycle between Ru^{4+} and Ru^{6+}. This cycle facilitates faster oxygen adsorption and deionization. Furthermore, RuO_2 exhibits excellent electrical conductivity, allowing quick electron transport and reducing resistance losses. [9]

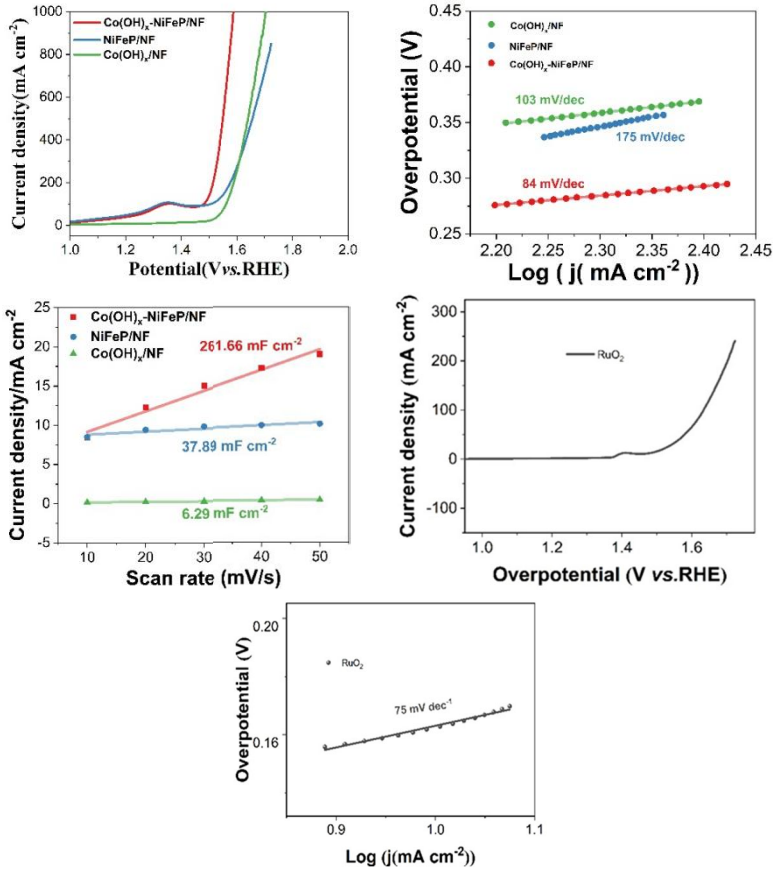

Fig. 4. (a) OER polarization curves of $Co(OH)_x$-NiFeP/NF, NiFeP/NF, and $Co(OH)_x$/NF. (b)Tafel slopes at 200 mA cm^{-2}. (c) Double-layer capacitance (Cdl) measurements. (d) OER polarization curves of RuO2. (e)Tafel slopes for RuO_2 at 200 mA cm^{-2}.

Electrochemical impedance spectroscopy (EIS) measurements and the corresponding equivalent circuit fitting results (Fig. 5a) indicated that the $Co(OH)_x$-NiFeP/NF catalyst exhibited the lowest charge transfer resistance at the interface of electrode and electrolyte, measured at 1.185 Ω, compared to the other catalysts. This significantly reduced resistance facilitates faster charge transfer and enhances OER kinetics. The improved interfacial charge transfer is likely due to the cooperative effect of the hierarchical structure and the crystalline-amorphous interface, which optimize the electronic conductivity and catalytic activity of $Co(OH)_x$-NiFeP/NF. The intrinsic catalytic activity of the active sites was quantitatively assessed using the turnover frequency (TOF) at an overpotential of 300 mV (1.53 V vs RHE), as shown in Fig. 5b. The $Co(OH)_x$-NiFeP/NF catalyst achieved a TOF of 0.87 s^{-1}, which is nearly twice that of NiFeP/NF (0.44 s^{-1}) and 3.5 times higher than that of $Co(OH)_x$/NF (0.25 s^{-1}). This significant enhancement in TOF underscores the superior intrinsic activity of $Co(OH)_x$-NiFeP/NF, further confirming its effectiveness in promoting the OER process. These results collectively demonstrate that Co(OH)x-NiFeP/NF possesses excellent interfacial charge transfer characteristics and exhibits higher intrinsic OER activity per active site compared to the other catalysts. The combination of low charge transfer resistance, high TOF, and robust performance under high current densities positions $Co(OH)_x$-NiFeP/NF as a promising and cost-effective alternative for OER applications in sustainable energy conversion technologies.[6-7]

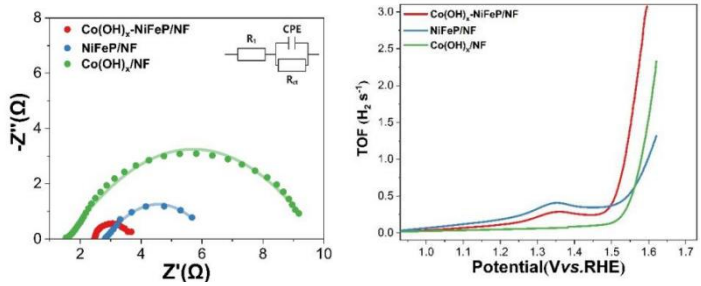

Fig. 5. (a) EIS Nyquist plots with equivalent circuit fitting. (b) TOF values of $Co(OH)_x$-NiFeP/NF, NiFeP/NF, and $Co(OH)_x$/NF at an overpotential of 300 mV.

The long-term durability of $Co(OH)_x$-NiFeP/NF was evaluated under high current density conditions, an important metric for practical applications of OER. Without iR compensation, the $Co(OH)_x$-NiFeP/NF catalyst maintained stable performance for over 200 hours, showing no significant decline in activity (see Fig. 6). This remarkable stability highlights its robustness and suitability for extended operation in energy-intensive applications. The OER activity and durability of $Co(OH)_x$-NiFeP/NF were superior to those of reference catalysts, emphasizing its exceptional performance. A comparative analysis with other high-current-density (HCD) OER catalysts further underscores the competitive advantage of $Co(OH)_x$-NiFeP/NF. The combination of excellent activity, prolonged stability, and structural integrity confirms $Co(OH)_x$-NiFeP/NF as a potential and cost-effective replacement for large-scale water-splitting systems.[5-7]

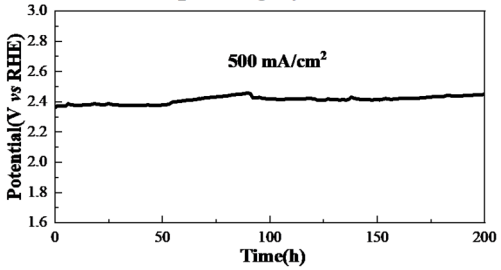

Fig. 6. Durability test of $Co(OH)_x$-NiFeP/NF under high current density conditions without iR compensation.

Given its good performance in both HER and OER, the practical application potential of $Co(OH)_x$-NiFeP/NF was further estimated in a two-electrode water electrolysis system, where $Co(OH)_x$-NiFeP/NF acted as both the cathode and anode (see Fig. 7). The uncorrected linear sweep voltammetry (LSV) curves for $Co(OH)_x$-NiFeP/NF || $Co(OH)_x$-NiFeP/NF and NiFeP/NF || NiCoP/NF in an alkaline electrolyte illustrate the overall water-splitting performance. At a current density of 10 mA cm^{-2}, $Co(OH)_x$-NiFeP/NF required a low voltage of just 1.51 V. In contrast, most reported bifunctional catalysts in the literature require voltages exceeding 1.69 V to achieve a current density of 100 mA cm^{-2}. Even at 1.7 V, many previously reported systems deliver current densities below 110 mA cm^{-2}.

In this study, the electrode achieved a current density of 100 mA cm^{-2} at a significantly lower voltage of 1.62 V, surpassing the performance of most catalysts until the day. At high current densities, $Co(OH)_x$-NiFeP/NF maintained excellent performance, requiring 1.74 V at 500 mA cm^{-2} and 1.84 V at 1000 mA cm^{-2}. A comparison of the performance of $Co(OH)_x$-NiFeP/NF with NiFeP/NF and other catalysts listed in Table 1 further demonstrates its superior efficiency under high current density (HCD) conditions. These findings highlight the exceptional dual-functional catalytic activity of $Co(OH)_x$-NiFeP/NF, establishing it as an up-and-coming candidate for large-scale alkaline water electrolysis systems.[8]

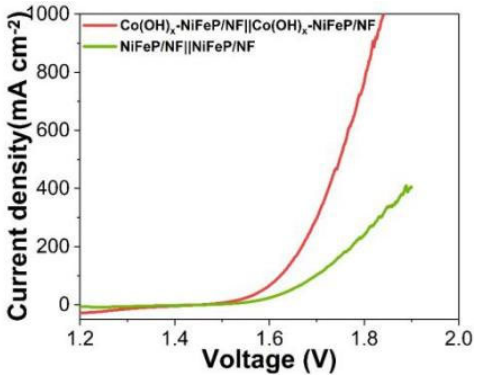

Fig. 7. LSV curves of $Co(OH)_x$-NiFeP/NF||$Co(OH)_x$-NiFeP/NF and NiFeP/NF||NiFeP/NF in an alkaline electrolyte.

Table 1. Comparative analysis of bifunctional water-splitting catalysts under high current density conditions.

catalysts	Current density (mA/cm2)	potential（V）
Co(OH)x-NiFeP/NF||Co(OH)x-NiFeP/NF	10	1.51
	500	1.74
	1000	1.84
NiFeP/NF||NiFeP/NF	10	1.55
	500	/
	1000	/

4. Comparison

In this study, we compared the electrocatalytic properties of $Co(OH)_x$-NiFeP/NF, $Co(OH)_x$/NF, NiFeP/NF, and RuO_2 in the OER. The experimental results indicate that the overpotential of $Co(OH)_x$-NiFeP/NF at 200 mA cm^{-2} is only 285 mV, which is much lower than the overpotentials of $Co(OH)_x$/NF (359 mV) and NiFeP/NF (347 mV). It even surpasses that of commercial RuO_2, which has an overpotential of 480 mV, demonstrating its superior catalytic activity. Furthermore, the Tafel slope of $Co(OH)_x$-NiFeP/NF is only 84 mV dec^{-1}, lower than the slopes for NiFeP/NF (175 mV dec^{-1}) and $Co(OH)_x$/NF (103 mV dec^{-1}). However, it is slightly higher than that of RuO_2 (75 mV dec^{-1}). This finding supports the excellent kinetics of oxygen evolution and the efficient charge transport capacity of $Co(OH)_x$-NiFeP/NF. Long-term stability tests demonstrate that $Co(OH)_x$-NiFeP/NF has outstanding durability, maintaining stable operation for 200 hours at a current density of 500 mA cm^{-2}. Its excellent catalytic performance is from the cooperative effect between $Co(OH)_x$ and NiFeP. $Co(OH)_x$ provides abundant active sites, while NiFeP enhances charge transfer and oxygen adsorption, significantly reducing the energy barrier for the oxygen evolution reaction. Despite its remarkable performance, $Co(OH)_x$-NiFeP/NF still slightly lags behind RuO_2 in terms of kinetics and stability. We speculate that incorporating appropriate dopants may help mitigate this limitation to some extent. In summary, $Co(OH)_x$-NiFeP/NF significantly outperforms the single-component catalysts in terms of catalytic activity, kinetic rate, and stability. Although it is slightly weaker than RuO_2 in kinetics and stability, it shows great potential as a replacement for precious metal catalysts and is expected to be applied in efficient and cost-effective hydrogen production technology through water electrolysis. In this study, we compared the electrocatalytic properties of $Co(OH)_x$-NiFeP/NF, $Co(OH)_x$/NF, NiFeP/NF, and RuO_2 in OER. The analyzed data indicate that the overpotential of $Co(OH)_x$-NiFeP/NF at 200 mA cm^{-2} is only 285 mV, which is highly smaller than the overpotentials of $Co(OH)_x$/NF (359 mV) and NiFeP/NF (347 mV). It even surpasses that of commercial RuO_2, which has an overpotential of 480 mV, demonstrating its superior catalytic activity. Furthermore, the Tafel slope of $Co(OH)_x$-NiFeP/NF is only 84 mV dec^{-1}, lower than the slopes for NiFeP/NF (175 mV dec^{-1}) and $Co(OH)_x$/NF (103 mV dec^{-1}). However, it is slightly higher than that of RuO_2 (75 mV dec^{-1}). This finding supports the excellent kinetics of oxygen evolution and the efficient charge transport capacity of $Co(OH)_x$-NiFeP/NF. Long-term stability tests demonstrate that $Co(OH)_x$-NiFeP/NF has outstanding durability and stable working for 200 hours at a current density of 500 mA cm^{-2}. Its excellent catalytic performance is because of the cooperative effect between $Co(OH)_x$ and NiFeP. $Co(OH)_x$ provides abundant active sites, while NiFeP enhances charge transfer and oxygen adsorption, significantly reducing the energy barrier for the oxygen evolution reaction. Despite its remarkable performance, $Co(OH)_x$-NiFeP/NF still slightly lags behind RuO_2 in terms of kinetics and stability. We speculate that incorporating appropriate dopants may help mitigate this limitation to some extent. In summary, $Co(OH)_x$-NiFeP/NF significantly outperforms the single-component catalysts in terms of catalytic activity, kinetic rate, and stability. Although it is slightly weaker than RuO_2 in kinetics and stability, it shows great potential as a replacement for precious metal catalysts and is expected to be applied in efficient and cost-effective hydrogen production technology through water electrolysis.

5. Conclusion

In this study, we developed a novel $Co(OH)_x$-NiFeP/NF catalyst characterized by a unique crystalline-amorphous structure, which demonstrated exceptional performance for water electrolysis at high current densities. Its hierarchical architecture features nanoneedles coated with amorphous $Co(OH)_x$, resulting in an enlarged surface area and increased charge transfer efficiency. This led to low overpotentials, superior intrinsic activity, and remarkable durability. The $Co(OH)_x$-NiFeP/NF catalyst exhibited an overpotential of 285 mV at a current density of 200 mA cm^{-2} and maintained stability for over 200 hours under high current conditions. Comparative studies highlighted the significantly improved catalytic performance of Co(OH)x-NiFeP/NF compared to NiFeP/NF and Co(OH)x/NF, which can be attributed to its optimized architecture and the synergistic effects at the crystalline-amorphous interface.

Furthermore, when applied in a full water-splitting electrolyzer, Co(OH)x-NiFeP/NF showed excellent efficiency, achieving 100 mA cm^{-2} at 1.62 V. This underscores its practical potential for sustainable energy applications. With low charge transfer resistance, high turnover frequency, and stability under extreme conditions, Co(OH)x-NiFeP/NF positions itself as a highly competitive and scalable catalyst for large-scale alkaline water electrolysis. This work states valuable idea and direction to the research of advanced bifunctional catalysts for next-generation energy systems.

References

[1] Wang, S., Lu, A., & Zhong, C.-J. (2021). Hydrogen production from water electrolysis: Role of catalysts. Nano Convergence, 8(4). https://doi.org/10.1186/s40580-021-00254-x

[2] Zhu, Y., Zhou, W., Yu, J., Chen, Y., & Shao, Z. (2019). Self-supported transition-metal-based electrocatalysts for hydrogen and oxygen evolution. Advanced Materials, 31(31), 1806326. https://doi.org/10.1002/adma.201806326

[3] Hu, F., Zhu, S., Chen, S., Li, Y., Ma, L., Wu, T., Zhang, Y., Wang, C., Liu, C., Yang, X., Song, L., & Xiong, Y. (2017). Amorphous metallic NiFeP: A conductive bulk material achieving high activity for oxygen evolution reaction in both alkaline and acidic media. Advanced Materials, 29(32), 1606570. https://doi.org/10.1002/adma.201606570

[4] Song, M., Zhang, Z., Li, Q., Jin, W., Wu, Z., Fu, G., & Liu, X. (2019). Ni-foam supported Co(OH)F and Co–P nanoarrays for energy-efficient hydrogen production via urea electrolysis. Journal of Materials Chemistry A, 7, 3697–3703. https://doi.org/10.1039/C8TA10985K

[5] Diao, F., Huang, W., Ctistis, G., Wackerbarth, H., Yang, Y., Si, P., Zhang, J., Xiao, X., & Engelbrekt, C. (2021). Bifunctional and self-supported NiFeP-layer-coated NiP rods for electrochemical water splitting in alkaline solution. ACS Applied Materials & Interfaces, 13(20), 23702–23713. https://doi.org/10.1021/acsami.1c03089

[6] Zhang, Y., Zhang, X., Li, H., Wang, Y., & Wang, Z. (2025). Facile synthesis of hierarchical $NiCo_2S_4$@NiFe LDH core–shell heterostructure on nickel foam for high-performance supercapacitors. Journal of Colloid and Interface Science, 600, 456–465. https://doi.org/10.1016/j.jcis.2025.02.099

[7] Kumar, A., & Singh, B. (2023). A study on synthesis and evaluation of catalytic activity of NiFeP nanosheets on. Neliti.https://www.neliti.com/publications/453496/a-study-on-synthesis-and-evaluation-of-catalytic-activity-of-nifep-nanosheets-on

[8] Zhang, X., Li, H., Wang, Y., & Wang, Z. (2022). CeO_2 nanoparticles decorated on porous Ni–Fe bimetallic phosphide nanosheets for high-efficient overall water splitting. Materials Research Letters, 10(7), 456–465. https://doi.org/10.1080/21663831.2022.2131372

[9] Bai, J., Zhou, W., Xu, J., Zhou, P., Deng, Y., Xiang, M., Xiang, D., & Su, Y. (2024). RuO_2 catalysts for electrocatalytic oxygen evolution in acidic media: Mechanism, activity promotion strategy and research progress. Molecules, 29(2), 537.https://doi.org/10.3390/molecules29020537MDPI+2